Clinical Cancer Research

Combination of YM155, a survivin suppressant, with bendamustine and rituximab: A new combination therapy to treat relapsed/refractory diffuse large B-cell lymphoma

Naoki Kaneko, Keisuke Mitsuoka, Nobuaki Amino, et al.

Clin Cancer Res Published OnlineFirst January 31, 2014.

Combination of YM155, a survivin suppressant, with bendamustine and rituximab: A new combination therapy to treat relapsed/refractory diffuse large B-cell lymphoma

Naoki Kaneko, Keisuke Mitsuoka, Nobuaki Amino, Kentaro Yamanaka, Aya Kita, Masamichi Mori, Sosuke Miyoshi and Sadao Kuromitsu

Drug Discovery Research, Astellas Pharma Inc., 21 Miyukigaoka, Tsukuba-shi, Ibaraki, Japan

Running Title: The efficacy of YM155/bendamustine/rituximab against DLBCL

Key words: Survivin, YM155, Bendamustine, Rituximab, DLBCL

Grant Support: none

Corresponding Author:

Naoki Kaneko

Drug Discovery Research, Astellas Pharma Inc., 21 Miyukigaoka Tsukuba-shi, Ibaraki, 305-8585 Japan

Tel: +81-29-829-6008

Fax: +81-29-852-2558

E-mail: naoki.kaneko@astellas.com

Disclosure of Potential Conflict of Interest

All authors are employees of Astellas Pharma, Inc. and have no other relevant conflicts of interest to disclose.

Word count: 4379 words

Number of figures: 4

Translational Relevance

While combination of bendamustine with rituximab is an effective therapy for relapsed/refractory DLBCL, the standard therapy for relapsed/refractory DLBCL has not been fully established. Here we found that the combination of YM155 with bendamustine showed synergistic effect through the inhibition of DNA damage repair responses as well as survivin accumulation at the G2/M phase in DLBCL cells. In a human DLBCL xenograft model, combination of YM155 with bendamustine induced complete tumor regression without exacerbating body weight loss. Further, the combination of YM155 with bendamustine and rituximab prolonged overall survival in an activated B-cell-like (ABC)-DLBCL disseminated xenograft model when compared with combination of bendamustine with rituximab. These results suggest that the combination of YM155 with bendamustine and rituximab might be a promising combination therapy for patients with relapsed/refractory DLBCL.

ABSTRACT

Purpose: There remains an unmet therapeutic need for patients with relapsed/refractory diffuse large B-cell lymphoma (DLBCL). The purpose of this study was to evaluate the therapeutic potential of sepantronium bromide (YM155), a survivin suppressant, in combination with either bendamustine or both bendamustine and rituximab using DLBCL models.

Experimental design: Human DLBCL cell lines: DB, SU-DHL-8 and WSU-DLCL2, were treated with YM155 in combination with bendamustine. Cell viability, apoptosis induction, protein expression, and cell cycle distribution were evaluated. Further, antitumor activities of YM155, in combination with bendamustine or both bendamustine and rituximab, were evaluated in mice bearing human DLBCL xenografts.

Results: The combination of YM155 with bendamustine showed greater cell growth inhibition and sub-G1 population than either agent alone. YM155 inhibited bendamustine-induced activation of the ATM pathway and accumulation of survivin at G2/M phase, with greater DNA damage and apoptosis than either single agent alone. In a DLBCL DB murine xenograft model, YM155 enhanced the antitumor activity of bendamustine, resulting in complete tumor regression without affecting body weight. Further, YM155 combined with bendamustine and rituximab, decreased FLT-PET signals in lymph nodes and prolonged overall survival of mice bearing disseminated SU-DHL-8, an activated B-cell-like (ABC)-DLBCL xenografts when compared with the combination of either rituximab and bendamustine or YM155 with rituximab.

Conclusions: These results support a clinical trial of the combination of YM155 with bendamustine and rituximab in relapsed/refractory DLBCL.

Introduction

Diffuse large B-cell lymphoma (DLBCL) is the most common type of non-Hodgkin's lymphoma (NHL). It accounts for approximately 30% to 40% of cases in adults (1). The anti-CD20 antibody rituximab (Rituxan®) is commonly used to treat many types of CD20-positive NHL, including DLBCL (2), and combination therapy of rituximab with standard cytotoxic chemotherapy regimens; such as R-CHOP (rituximab plus cyclophosphamide, hydroxydoxorubicin, vincristine, and prednisone), is the current standard of care for B-cell NHL (3-5). However, approximately 30% of the patients either do not respond to or develop resistance to further treatment, and approximately half of relapsed patients are not eligible for high-dose chemotherapy, following autologous stem cell transplantation (6). Therefore, the development of effective and well-tolerated therapies for elderly, frail, relapsed, or refractory DLBCL patients represents an unmet clinical need.

Bendamustine, a bifunctional alkylating agent containing a nitrogen mustard moiety chemically linked to a purine analogue, is approved treating multiple hematological tumors, including indolent and rituximab-resistant NHL (7). In large-scale screenings, such as the National Cancer Institute (NCI) In Vitro Cell Line Screening Project and gene microarrays, bendamustine showed a unique mechanistic profile, which included activation of DNA damage stress responses and apoptosis, inhibition of mitotic checkpoints, and induction of mitotic catastrophe, when compared with most other conventional alkylators such as cyclophosphamide and melphalan (8). Further, bendamustine exhibited limited cross-resistance to other alkylating agents and showed prolonged effects towards DNA damage (9). *In vitro*, CD20-positive DLBCL and primary chronic lymphocytic leukemia (CLL) cell lines showed a synergistic effect toward the combination use of bendamustine with rituximab (10). Further, the

combination of bendamustine with rituximab is reported to have superior efficacy and tolerability in indolent B-cell NHL patients as compared with R-CHOP (11) and showed clinical activity (overall response rate: 62.7%; complete response [CR]: 37.3%, partial response [PR]: 25.4%) in patients with relapsed/refractory DLBCL in a phase II study (12). As such, this combination was suggested as a second-line therapy for DLBCL according to the National Comprehensive Cancer Network (NCCN) guidelines (version 1, 2013) (13). Together, the findings suggest that the combination of bendamustine with rituximab would be an effective therapy for relapsed/refractory DLBCL.

Survivin is a member of the inhibitor of apoptosis protein family and has been implicated in both cell survival and regulation of mitosis in cancer (14). Its overexpression has been associated with chemoresistance and a poor clinical outcome in cancer patients, including DLBCL (15-17). As well, survivin inhibition has been demonstrated to sensitize tumors to cytotoxic drugs including taxanes, etoposide, mitomycin C and cisplatin *in vitro* and *in vivo* (18-20). Although cancer cells can acquire resistance to apoptosis through various mechanisms, it is suggested that tumor cells may acquire a cytoprotective phenotype by mitigating apoptosis induction through overexpression of survivin.

Sepantronium bromide (YM155) is a selective survivin suppressant, which demonstrates potent antitumor activities against a wide range of cancers in various mouse models of tumor xenografts, including NHL (21-23). The combination of YM155 with rituximab also showed greater antitumor activity, and resulted in longer survival than each single agent alone (24). In a phase I study, three of five patients with NHL, including one with DLBCL refractory to R-CHOP, showed an objective response to single agent YM155 (25). A phase II trial confirmed the safety and tolerability of YM155 in patients with refractory DLBCL (26). In another phase II trial, the combination of YM155 with rituximab also showed

clinical activity (interim data: overall response rate 9/16 [56.3%], with 2/16 [12.5%] CR, 7/16 [43.8%] PR, and 4/16 [25%] stable disease [SD]) (27). These findings suggested that YM155 was clinically active against DLBCL, when combined with rituximab.

Given the above, we hypothesized that a triple combination of YM155 with bendamustine and rituximab would show enhanced antitumor activity when compared to the combination of these two agents alone against DLBCL. Here, we examined the antitumor activity of YM155 in combination with bendamustine against DLBCL models both *in vitro* and *in vivo*. We also investigated the life-prolonging effect of YM155 in combination with bendamustine and rituximab in a disseminated DLBCL xenograft model.

Materials and Methods

Cell culture

The human DLBCL cell line DB was purchased from the American Type Culture Collection (Manassas, VA, USA). The human DLBCL cell lines; WSU-DLCL2 and SU-DHL-8 were purchased from the German Resource Center for Biological Material (DSMZ, Braunschweig, Germany). Cells were cultured at 37 °C in a 5% CO_2 atmosphere in RPMI 1640 medium supplemented with 10% heat-inactivated fetal bovine serum (Sigma-Aldrich, St. Louis, MO, USA). All cell lines were authenticated by Short Tandem Repeat profiling (Promega, Madison, WI, USA).

Reagents and antibodies

Sepantronium bromide (YM155) was synthesized at Astellas Pharma Inc. (Tokyo, Japan), dissolved in dimethyl sulfoxide (DMSO), and diluted with culture medium. Rituximab and bendamustine were purchased from Genentech Inc. (San Francisco, CA, USA) and Sigma-Aldrich, respectively, and dissolved in phosphate buffered saline (PBS). For *in vivo* studies, bendamustine hydrochloride (Levact®), hereafter referred to as "bendamustine", was purchased from Mundipharma (Limburg, Germany). The doses of YM155 and bendamustine were expressed in terms of free base of each drug substance. All drugs were dissolved and diluted in saline just before administration. Anti-survivin antibody was purchased from R&D Systems Inc. (Minneapolis, MN, USA); phosho-ATM (S1981), phosho-p53 (S15), phosho-chk2 (T68), phospho-histone H2AX (S139), and phosho-cdc2 (Y15) from Cell Signaling Technology Inc. (Danvers, MA, USA); and β-actin from Sigma-Aldrich.

***In vitro* assay for cell viability**

Cell viability was determined using a CellTiter-Fluor® Cell Viability Assay (Promega). The fluorescence of each sample was measured using an Infinite® 200 PRO (Tecan Group Ltd., Männedorf, Switzerland). Assays were performed in triplicate, and mean values were obtained based on the results of three independent assays.

Western blot analysis

Protein was extracted using lysis buffer (RIPA Buffer [Thermo Fisher Scientific, Waltham, MA, USA], 1 × Halt phosphatase inhibitor cocktail [Thermo Fisher Scientific] and protease inhibitor cocktail [Sigma-Aldrich]). Protein concentrations of the lysates were determined using a BCA protein assay reagent kit (Thermo Fisher Scientific). Equal amounts of total protein were resolved by SDS-PAGE and transferred to a polyvinylidene fluoride (PVDF) membrane. After blocking at room temperature with Blocking One (Nacalai Tesque, Kyoto, Japan), each membrane was incubated overnight at 4 °C with the primary antibodies. After washing with TBS-T, membranes were incubated with HRP-conjugated secondary antibody for 1 h at room temperature. Proteins of interest were visualized by enhanced chemiluminescence using ECL-Prime (GE Healthcare, Fairfield, CT, USA).

Cell cycle analysis

Cell cycle distribution was determined using a Guava PCA microcytometer (Guava Technologies, Hayward, CA, USA). Cells were fixed with ice-cold 70% ethanol and incubated at 4 °C. Ethanol-fixed cells were washed with PBS and resuspended in Guava Cell Cycle Reagent (Guava Technologies). For

data collection, 5000 events were acquired per sample and analyzed using CytoSoft software (Guava Technologies). Mean values were obtained from three independent assays.

Subcutaneous xenograft model

All animal experimental procedures were approved by the Institutional Animal Care and Use Committee of Astellas Pharma, Inc., and the Tsukuba Research Center of Astellas Pharma, Inc., is accredited by AAALAC International. Four-week-old male nude mice (CAnN.Cg-Foxn1nu/CrlCrlj [nu/nu]) were obtained from Charles River Japan (Kanagawa, Japan). DB cells were mixed with Matrigel® (BD Biosciences, MA, USA), and 3×10^6 cells were subcutaneously (s.c.) injected into the flanks of mice. After tumor development, 32 mice were divided into 4 groups of 8 based on tumor volume, with almost equal body weights across all groups. The first day of drug administration was designated as d 0, and observation continued until d 21. YM155 was administered at 1 mg/kg/day by continuous s.c. infusion for 7 days using a micro-osmotic pump (Alzet® model 1007D; Durect, Cupertino, CA, USA). Bendamustine at 50 mg/kg was administered intravenously (i.v.) once on d 0. Body weight and tumor diameter were measured twice a week, and tumor volume was determined (length × width^2 × 0.5). Complete regression (CR) was defined as tumor regression to below the limit of palpation. The percent inhibition of tumor growth on d 21 was calculated for each group using the following formula:

100 × (1 – {mean [(tumor volume of each mouse on d 21) − (tumor volume of each mouse on d 0)] of each group} / {mean [(tumor volume of each mouse on d 21) − (tumor volume of each mouse on d 0)] of the control group})

When the percent inhibition of tumor growth exceeded 100%, the percent of tumor regression was

calculated using the following formula:

100 × [1 − (mean tumor volume of each group on d 21) / (mean tumor volume of each group on d 0)]

Disseminated xenograft model

Five-week-old male severe combined immunodeficient (SCID) mice (CB17/Icr-Prkdcscid/CrlCrlj) were purchased from Charles River Japan. SU-DHL-8 cells were injected i.v. (1×10^6 cells/0.1 mL/mouse), and dissemination and tumor growth was allowed to proceed for 14 days. The mice were then divided into 5 comparable groups of 10 animals each based on body weight using SAS software (SAS Institute, Cary, NC, USA). YM155 (1 mg/kg continuous s.c. infusion for 7 days starting on d 0 and d 19), rituximab (50 mg/kg i.v. on d 0, 2, 19, and 22), and bendamustine (25 mg/kg i.v. on d 0, 1, 19, and 20) were administered as double combination (YM155 plus rituximab) or triple combination (YM155 plus rituximab plus bendamustine), and the condition of animals was monitored daily. Mice were scored as dead if any of the following signs of suffering were observed: cachexia, weakening, and difficulty moving or eating. Mice scored as dead were euthanized while under diethyl ether anesthesia.

^{18}F-3'-fluoro-3' deoxythymidine positron emission tomography (^{18}F-FLT-PET) imaging

^{18}F-FLT was synthesized in-house from its precursors as described previously (24). The specific activity of ^{18}F-FLT exceeded 45.1 MBq/nmol (1.22 Ci/μmol) at the end of synthesis. For imaging studies, we used 5 mice per group for each independent experiment. Treatment regimens were the same as described above. ^{18}F-FLT uptake was evaluated using an Inveon docked PET/CT system (Siemens, Knoxville, TN, USA) on d 16 of treatment. Mice were fasted for over 18 h prior to imaging. For imaging, 9.8-11.8 MBq aliquots of ^{18}F-FLT were administered via tail vein injection to conscious animals that were

subsequently maintained in cages for 1 h to allow for ^{18}F-FLT uptake into tumors. Mice were anesthetized with 2.0%-2.5% isoflurane/O_2 gas and placed in a mouse imaging chamber (m2m Imaging Corp, Cleveland, OH, USA). A 5-min emission scan was performed using the PET scanner followed by CT imaging (500 μA, 80 kV). Regions of interest (ROI) were drawn around the boundaries of tumors in lymph nodes on coronal slices, and the observed maximum pixel value was normalized to the injected dose and body weight to give the maximum standardized uptake value (SUV_{max}).

Analysis for synergy

The Bliss additivism model (28, 29) was used to classify the effect of combining two agents as additive, synergistic, or antagonistic. A theoretical curve was calculated for combined inhibition using the equation E_{bliss}: bliss index = $E_A + E_B - E_A \times E_B$, where E_A and E_B are the fractional inhibitions obtained by drug A alone and drug B alone at specific concentrations. The combined effect of the two drugs was judged as follows, $E_{A+B} > E_{bliss}$: synergistic, $E_{A+B} = E_{bliss}$: additive, and $E_{A+B} < E_{bliss}$: antagonistic.

Statistical analysis

Values were expressed as mean ± standard error of the mean (SEM). Tumor volume and body weight on d 21 were compared between each single compound group and the combination group by using Student's t-test with SAS software (SAS Institute, Cary, NC, USA). For PET study, Quantitative ROI analysis was conducted by applying Student's t-test with GraphPad Prism (GraphPad Software, San Diego, CA, USA). For survival analysis, Kaplan-Meier curves were generated, and differences were assessed using log-rank test with GraphPad Prism. *P*-values less than 0.05 were considered significant.

Results

Effect of YM155 in combination with bendamustine in DLBCL cell lines *in vitro*

We first evaluated the *in vitro* combined effect of YM155 with bendamustine in DLBCL cell lines. YM155 at 10 nmol/L combined with bendamustine (250 μmol/L for DB cells, 100 μmol/L for SU-DHL-8 cells, and 150 μmol/L for WSU-DLCL2 cells) were treated for 24 h or 48 h and assessed for cell viability and apoptosis induction, respectively. The combination of YM155 with bendamustine induced a greater decrease in cell viability than either agent alone. The percentages of cell growth inhibition, induced by YM155, bendamustine, combination of both agents, and bliss index were 14%, 54%, 86%, and 61% in DB cells; 39%, 39%, 82%, and 70% in SU-DHL-8 cells; and 46%, 54%, 93% and 86% in WSU-DLCL2 cells, respectively (Figure 1A). The combination induced a greater sub-G1 population, indicative of apoptosis, than either agent alone. The percentages of sub-G1 population induced by YM155, bendamustine, and combination of both were 5.9%, 6.5%, and 27% in DB cells; 19%, 32%, and 58% in SU-DHL-8 cells; and 46%, 30%, and 71% in WSU-DLCL2 cells, respectively (Figure 1B).

Antitumor effects of YM155 combined with bendamustine in a DB xenograft model

The efficacy of YM155 in combination with bendamustine was examined in a DB human DLBCL xenograft model. YM155 treatment alone via continuous s.c. infusion at 1 mg/kg/day for 7 days inhibited tumor growth by 97% with CR in 1 out of 8 mice with DB xenografts. Bendamustine treatment alone, via single i.v. bolus injection at 50 mg/kg, induced tumor regression by 24%, with CR in 2 out of 8 mice (Figure 2A). The combination of YM155 with bendamustine induced tumor regression by 99%. As well, the combination treatment led to CR in 6 out of 8 mice. No significant decrease in body weight was

observed in the combination treatment group as compared to each single treatment group (Figure 2B).

Mechanisms of action for combination of YM155 with bendamustine

Bendamustine is reported to induce DNA damage, which activated the Ataxia Telangiectasia Mutated Protein (ATM) pathway and G2/M arrest in multiple myeloma cells (30). To investigate the mechanisms of action for the combination of YM155 with bendamustine, we examined the status of the ATM pathway as well as changes in cell cycle status. Treatment with bendamustine induced DNA damage indicated by phospho-histone H2AX (γ-H2AX), a marker of DNA double strand breaks. In response to DNA damage, bendamustine induced phosphorylation of ATM and its substrates, including p53 and check point kinase-2 (chk2), which leads to phosphorylation of cdc2 in DB cells. Bendamustine also increased the G2/M phase population and accumulated survivin in DB cells (Figure 3). The combined treatment of YM155/bendamustine decreased bendamustine-induced phosphorylation of ATM, p53, chk2, and cdc2, and accumulated survivin; resulting in a greater amount of γ-H2AX and cleaved PARP and a larger sub-G1 population than can be achieved with either single agent alone (Figure 3).

Life-prolonging effect of YM155 in combination with bendamustine and rituximab in a SU-DHL-8 disseminated xenograft model

The combination of bendamustine with rituximab is reported to be effective against relapsed/refractory DLBCL. To evaluate whether YM155 can enhance the efficacy of bendamustine in combination with rituximab, we examined the survival benefit of YM155 in combination with bendamustine and rituximab in a SU-DHL-8 disseminated xenograft model. FLT-PET images visualized lymph node infiltration

(submandibular, axillary, and inguinal lymph nodes), which was found in 100% of non-treated mice on 30 days after cancer cell inoculation. All mice bearing lymphoma showed multiple infiltrated lymphatic regions, being >4. No bone marrow infiltration was detected (Figure S2A). In the triple combination group, PET signals in lymph nodes were decreased. Quantitative ROI analysis indicated that, in submandibular and inguinal lymph nodes of animals in the triple treatment group, the signals were significantly smaller than those found in the non-treatment group (Figure 2SB). The administration of YM155 alone, bendamustine combined with rituximab, or YM155 combined with rituximab extended the median survival from 45.5 to 68, 57.5, and 78 days, respectively. Further, the triple treatment combination: YM155/bendamustine/rituximab, significantly prolonged survival as compared with respective YM155 alone, bendamustine combined with rituximab, or YM155 combined with rituximab treatments (Figure 4). The median survival in the triple combination treatment group was 86 days.

Discussion

Here, we examined the therapeutic potential of YM155 in combination with bendamustine or bendamustine/rituximab against DLBCL both *in vitro* and *in vivo*. The intrinsic survivin in tested DLBCL cell lines is highly expressed (Figure S1). We found that the combination of YM155 with bendamustine decreased cell viability to a greater extent than either single agent alone. Bliss additivism analysis revealed that the combined effect was synergistic (Figure 1A). The combination of YM155 with bendamustine induced greater apoptosis in DLBCL cell lines than either single agent alone (Figure 1B). Similar results were obtained in multiple drug concentrations (data not shown). Further, this combination induced greater antitumor activity, including complete regression, than either single agent in a DB DLBCL xenograft model without affecting body weight (Figure 2). Together, the results suggest that YM155 combined with bendamustine is effective for treating of DLBCL.

Bendamustine is reported to have multiple modes of action. Primarily, bendamustine has been shown to form DNA cross-links, that induces DNA damage and results in activating the ATM pathway (8, 30). The ATM pathway is a central pathway to repair of DNA double strand break (DNA-DSBs) in DNA, thereby influencing genome stability and cell survival. ATM is a major regulator of the DNA damage response by activation of chk2, and p53 and leads to induction of response genes involved in cell cycle arrest, DNA repair, and/or apoptosis (31). Secondarily, bendamustine also inhibits mitotic checkpoints and induces G2/M arrest (8, 30). The expression of survivin is regulated in a cell cycle-dependent manner and peaks at mitosis (32). We showed that bendamustine induced DNA damage, activated the ATM pathway, and phosphorylated cdc2, resulting in G2/M arrest accompanied by accumulating survivin protein in DLBCL cells. In addition, the combined treatment of YM155 and

bendamustine inhibited the bendamustine-induced activation of the ATM pathway and increased survivin expression, consequently promoting DNA damage and apoptosis than either single agent alone (Figure 3A). Survivin is known to be radiation resistance factor in tumor cells (33). The expression of survivin was increased by ionizing radiation through chk2 activation in breast and colon cancer cells (34). Further, survivin is reported to be linked to DNA-DSB repair by interaction with members of the DNA-DSB repair machinery (35). Survivin siRNA impaired irradiation-induced DNA-DSB repair, as demonstrated by an increase of γ-H2AX, and resulted in increased apoptosis (35, 36). YM155 is known to sensitize NSCLC cells to radiation and platinum agents both *in vitro* and *in vivo,* through the inhibition of DNA damage repair (37, 38). As well, we demonstrated that survivin suppression by YM155 enhances the antitumor activity of docetaxel through the inhibition of survivin accumulation at G2/M in NSCLC (39) and melanoma cells (40). Taken together, these results suggest that survivin suppression by YM155 enhances the antitumor activity of bendamustine through the inhibition of DNA damage repair responses as well as survivin-mediated cytoprotection at the G2/M phase.

In our previous studies, the combination of YM155 with rituximab exhibited a synergistic effect against B-cell NHL, including DLBCL (24), and STAT3 inhibition by rituximab contributed to the synergistic effect seen in WSU-DLCL2 and SU-DHL-4 DLBCL cell lines (41), which suggested the possibility that YM155 would enhance the antitumor effect of bendamustine when combined with rituximab through different mechanisms in DLBCL. In the present study, we examined the life-prolonging effect of YM155 in combination with bendamustine and rituximab in a SU-DHL-8 disseminated xenograft model. DLBCL commonly develops clinically as disseminated disease (42), and in this model, dissemination of tumors in lymph nodes was detected using ^{18}F-FLT-PET (Figure 2SA).

Activated B-cell-like DLBCL has been reported to be more resistant to CHOP or R-CHOP than germinal center B-cell-like DLBCL (GCB-DLBCL) (43, 44). In preliminary studies, we confirmed that R-CHOP did not show antitumor activity against SU-DHL-8, an ABC-DLBCL xenografts (45) but did show antitumor activity against DB, GCB-DLBCL xenografts (data not shown). These facts indicate that this model recapitulates many features found in refractory DLBCL patients. In this model, the triple combination treatment resulted in decreased FLT-PET signals in lymph nodes (Figure 2S) and in significantly longer overall survival than either YM155 alone, or the combination of bendamustine with rituximab, or the combination of YM155 with rituximab (Figure 4). In addition, the concentration of YM155 used here (1 mg/kg/day) can be clinical achieved concentration (21, 46). The results suggest that the triple combination of YM155 with bendamustine and rituximab is expected to exert greater clinical benefits in patients with relapsed/refractory DLBCL than the sole combination of these two agents. In clinical settings, the combination of bendamustine with rituximab is a promising salvage regimen for patients with relapsed/refractory DLBCL after rituximab-containing chemotherapy. Despite its clinical benefits, the high dose bendamustine treatment was often limited due to development of hematologic toxicity, primarily lymphopenia, neutropenia, leukopenia, and thrombocytopenia (12). YM155 monotherapy demonstrated modest anticancer activity with no serious hematologic events in patients with refractory DLBCL (26). These data suggest that the combination of YM155 with bendamsutine and rituximab may be beneficial. However, further clinical investigation will be required to verify the tolerability and therapeutic potential of this triple combination regimen against relapsed/refractory DLBCL.

In conclusion, here we have shown that YM155 enhances the antitumor activity of bendamustine against DLBCL models through inhibition of DNA damage responses as well as survivin-mediated cytoprotection at the G2/M phase. Further, the triple combination of YM155 with bendamustine and rituximab showed superior survival benefit as compared to double treatments. These data prompt further clinical investigations of YM155 in combination with bendamustine and rituximab for the treatment of relapsed/refractory DLBCL.

Figure legend

Figure 1. Effect of combined treatment with YM155 and bendamustine on cell proliferation and apoptosis induction in DLBCL cell lines.

DB, SU-DHL-8, and WSU-DLCL2 cells were treated with YM155, in combination with bendamustine, (BEN) at indicated concentrations. (A) After treatment for 24 h, cell viability was determined using a CellTiter-Fluor® Cell Viability Assay. The fluorescent value of treated cells was normalized to that of DMSO control and is shown as % inhibition of vehicle control. Each point represents the mean ± SEM from three independent assays. The mean of bliss index (representing the theoretical expectation if the combined effects of YM155 with bendamustine was exactly additive) from three independent assay was also showed as dashed line. (B) After treatment for 48 h, cells were harvested and sub-G1 populations were determined by flow cytometry. Each bar represents the mean ± SEM of the sub-G1 population from three separate experiments.

Figure 2. Antitumor activity of YM155 in combination with bendamustine against DB xenografts.

Tumor volume (A) and body weight (B) are expressed as the mean ± SEM (n=8). Mice received a continuous s.c. infusion of YM155 at 1 mg/kg/day for 7 days starting on d 0. Bendamustine was administered via i.v. bolus injection at 50 mg/kg on d 0. Tumor volume and body weight on d 21 were compared between each single compound group and the combination group using Student's t-test. *: $P<0.05$ versus bendamustine group, #: $P<0.05$ versus YM155 group, N.S.: not significantly different.

Figure 3. Mechanisms of action for combination of YM155 with bendamustine in DB cells. DB cells were treated with YM155 at 10 nmol/L, bendamustine (BEN) at 250 μmol/L, or both compounds (YM155 + BEN). (A) After treatment for 16 h, whole cell lysates were subjected to Western blotting using indicated antibodies. (B) After treatment for 48 h, cells were harvested, and cell cycle distribution was determined via flow cytometry.

Figure 4. Life-prolonging effect of combined treatment with YM155, bendamustine, and bendamustine (Y+B+R) in a SU-DHL-8 disseminated xenograft model. Animals (n=10/group) were monitored daily for survival. Statistical differences were determined by using the log-rank test. ** $P < 0.05$ versus YM155-rituximab (Y+R) combination group. ### $P < 0.001$ versus YM155 alone (Y) or bendamustine-rituximab (B+R) combination group. NT: no treatment.

Acknowledgements

We thank Y. Sawabe (KAC Co., Ltd., Kyoto, Japan) for help with the survival study; T. Kimura (Astellas Research Technology, Inc.) and J. Mizusawa (KAC Co., Ltd., Kyoto, Japan) for help with PET imaging studies; Dr. J. Grierson (University of Washington) for critical reading of the manuscript.

Authors' Contributions

N.K., K.M., N.A. designed, performed, analyzed research and wrote the manuscript. K.Y., A.K., M.M., S.M., and S.K. were responsible for research design and finalized the manuscript.

References

1. A clinical evaluation of the International Lymphoma Study Group classification of non-Hodgkin's lymphoma. The Non-Hodgkin's Lymphoma Classification Project. Blood. 1997;89:3909-18.

2. Cheson BD, Leonard JP. Monoclonal antibody therapy for B-cell non-Hodgkin's lymphoma. N Engl J Med. 2008;359:613-26.

3. Coiffier B, Lepage E, Briere J, Herbrecht R, Tilly H, Bouabdallah R, et al. CHOP chemotherapy plus rituximab compared with CHOP alone in elderly patients with diffuse large-B-cell lymphoma. N Engl J Med. 2002;346:235-42.

4. Hiddemann W, Kneba M, Dreyling M, Schmitz N, Lengfelder E, Schmits R, et al. Frontline therapy with rituximab added to the combination of cyclophosphamide, doxorubicin, vincristine, and prednisone (CHOP) significantly improves the outcome for patients with advanced-stage follicular lymphoma compared with therapy with CHOP alone: results of a prospective randomized study of the German Low-Grade Lymphoma Study Group. Blood. 2005;106:3725-32.

5. Pfreundschuh M, Trumper L, Osterborg A, Pettengell R, Trneny M, Imrie K, et al. CHOP-like chemotherapy plus rituximab versus CHOP-like chemotherapy alone in young patients with good-prognosis diffuse large-B-cell lymphoma: a randomised controlled trial by the MabThera International Trial (MInT) Group. Lancet Oncol. 2006;7:379-91.

6. Friedberg JW. Relapsed/refractory diffuse large B-cell lymphoma. Hematology Am Soc Hematol Educ Program. 2011;2011:498-505.

7. Garnock-Jones KP. Bendamustine: a review of its use in the management of indolent

non-Hodgkin's lymphoma and mantle cell lymphoma. Drugs. 2010;70:1703-18.

8. Leoni LM, Bailey B, Reifert J, Bendall HH, Zeller RW, Corbeil J, et al. Bendamustine (Treanda) displays a distinct pattern of cytotoxicity and unique mechanistic features compared with other alkylating agents. Clin Cancer Res. 2008;14:309-17.

9. Strumberg D, Harstrick A, Doll K, Hoffmann B, Seeber S. Bendamustine hydrochloride activity against doxorubicin-resistant human breast carcinoma cell lines. Anticancer Drugs. 1996;7:415-21.

10. Rummel MJ, Chow KU, Hoelzer D, Mitrou PS, Weidmann E. In vitro studies with bendamustine: enhanced activity in combination with rituximab. Semin Oncol. 2002;29:12-4.

11. Rummel MJ, Niederle N, Maschmeyer G, Banat GA, von Grunhagen U, Losem C, et al. Bendamustine plus rituximab versus CHOP plus rituximab as first-line treatment for patients with indolent and mantle-cell lymphomas: an open-label, multicentre, randomised, phase 3 non-inferiority trial. Lancet. 2013;381:1203-10.

12. Ohmachi K, Niitsu N, Uchida T, Kim SJ, Ando K, Takahashi N, et al. Multicenter phase II study of bendamustine plus rituximab in patients with relapsed or refractory diffuse large B-cell lymphoma. J Clin Oncol. 2013;31:2103-9.

13. NCCN Guidelines. 2013 July 3 [cited; Available from: http://www.nccn.org/clinical.asp

14. Mita AC, Mita MM, Nawrocki ST, Giles FJ. Survivin: key regulator of mitosis and apoptosis and novel target for cancer therapeutics. Clin Cancer Res. 2008;14:5000-5.

15. Adida C, Haioun C, Gaulard P, Lepage E, Morel P, Briere J, et al. Prognostic significance of survivin expression in diffuse large B-cell lymphomas. Blood. 2000;96:1921-5.

16. Markovic O, Marisavljevic D, Cemerikic V, Perunicic M, Savic S, Filipovic B, et al. Clinical

and prognostic significance of apoptotic profile in patients with newly diagnosed nodal diffuse large B-cell lymphoma (DLBCL). Eur J Haematol. 2011;86:246-55.

17. Ambrosini G, Adida C, Altieri DC. A novel anti-apoptosis gene, survivin, expressed in cancer and lymphoma. Nat Med. 1997;3:917-21.

18. Kunze D, Erdmann K, Froehner M, Wirth MP, Fuessel S. siRNA-mediated inhibition of antiapoptotic genes enhances chemotherapy efficacy in bladder cancer cells. Anticancer Res. 2012;32:4313-8.

19. Hayashi N, Asano K, Suzuki H, Yamamoto T, Tanigawa N, Egawa S, et al. Adenoviral infection of survivin antisense sensitizes prostate cancer cells to etoposide in vivo. Prostate. 2005;65:10-9.

20. Mesri M, Wall NR, Li J, Kim RW, Altieri DC. Cancer gene therapy using a survivin mutant adenovirus. J Clin Invest. 2001;108:981-90.

21. Nakahara T, Takeuchi M, Kinoyama I, Minematsu T, Shirasuna K, Matsuhisa A, et al. YM155, a novel small-molecule survivin suppressant, induces regression of established human hormone-refractory prostate tumor xenografts. Cancer Res. 2007;67:8014-21.

22. Nakahara T, Kita A, Yamanaka K, Mori M, Amino N, Takeuchi M, et al. Broad spectrum and potent antitumor activities of YM155, a novel small-molecule survivin suppressant, in a wide variety of human cancer cell lines and xenograft models. Cancer Sci. 2011;102:614-21.

23. Kita A, Nakahara T, Yamanaka K, Nakano K, Nakata M, Mori M, et al. Antitumor effects of YM155, a novel survivin suppressant, against human aggressive non-Hodgkin lymphoma. Leuk Res. 2011;35:787-92.

24. Kita A, Mitsuoka K, Kaneko N, Nakata M, Yamanaka K, Jitsuoka M, et al. Sepantronium

bromide (YM155) enhances response of human B-cell non-Hodgkin lymphoma to rituximab. J Pharmacol Exp Ther. 2012;343:178-83.

25. Tolcher AW, Mita A, Lewis LD, Garrett CR, Till E, Daud AI, et al. Phase I and pharmacokinetic study of YM155, a small-molecule inhibitor of survivin. J Clin Oncol. 2008;26:5198-203.

26. Cheson BD, Bartlett NL, Vose JM, Lopez-Hernandez A, Seiz AL, Keating AT, et al. A phase II study of the survivin suppressant YM155 in patients with refractory diffuse large B-cell lymphoma. Cancer. 2012;118:3128-34.

27. Papadopoulos KP. A Phase II Study of Sepantronium Bromide (YM155) Plus Rituximab in Previously Treated Subjects with Aggressive CD20-Positive B Cell Non-Hodgkin's Lymphoma Who Are Ineligible for or Have Previously Received an Autologous Stem Cell Transplant - Stage I Results. American Society of Hematology Annual meeting Abstract No 2731. 2012.

28. Berenbaum MC. Criteria for analyzing interactions between biologically active agents. Adv Cancer Res. 1981;35:269-335.

29. Buck E, Eyzaguirre A, Brown E, Petti F, McCormack S, Haley JD, et al. Rapamycin synergizes with the epidermal growth factor receptor inhibitor erlotinib in non-small-cell lung, pancreatic, colon, and breast tumors. Mol Cancer Ther. 2006;5:2676-84.

30. Gaul L, Mandl-Weber S, Baumann P, Emmerich B, Schmidmaier R. Bendamustine induces G2 cell cycle arrest and apoptosis in myeloma cells: the role of ATM-Chk2-Cdc25A and ATM-p53-p21-pathways. J Cancer Res Clin Oncol. 2008;134:245-53.

31. Shiloh Y. ATM and related protein kinases: safeguarding genome integrity. Nat Rev Cancer. 2003;3:155-68.

32. Li F, Ambrosini G, Chu EY, Plescia J, Tognin S, Marchisio PC, et al. Control of apoptosis and mitotic spindle checkpoint by survivin. Nature. 1998;396:580-4.

33. Chakravarti A, Zhai GG, Zhang M, Malhotra R, Latham DE, Delaney MA, et al. Survivin enhances radiation resistance in primary human glioblastoma cells via caspase-independent mechanisms. Oncogene. 2004;23:7494-506.

34. Ghosh JC, Dohi T, Raskett CM, Kowalik TF, Altieri DC. Activated checkpoint kinase 2 provides a survival signal for tumor cells. Cancer Res. 2006;66:11576-9.

35. Reichert S, Rodel C, Mirsch J, Harter PN, Tomicic MT, Mittelbronn M, et al. Survivin inhibition and DNA double-strand break repair: a molecular mechanism to overcome radioresistance in glioblastoma. Radiother Oncol. 2011;101:51-8.

36. Rodel F, Hoffmann J, Distel L, Herrmann M, Noisternig T, Papadopoulos T, et al. Survivin as a radioresistance factor, and prognostic and therapeutic target for radiotherapy in rectal cancer. Cancer Res. 2005;65:4881-7.

37. Iwasa T, Okamoto I, Takezawa K, Yamanaka K, Nakahara T, Kita A, et al. Marked anti-tumour activity of the combination of YM155, a novel survivin suppressant, and platinum-based drugs. Br J Cancer. 2010;103:36-42.

38. Iwasa T, Okamoto I, Suzuki M, Nakahara T, Yamanaka K, Hatashita E, et al. Radiosensitizing effect of YM155, a novel small-molecule survivin suppressant, in non-small cell lung cancer cell lines. Clin Cancer Res. 2008;14:6496-504.

39. Nakahara T, Yamanaka K, Hatakeyama S, Kita A, Takeuchi M, Kinoyama I, et al. YM155, a novel survivin suppressant, enhances taxane-induced apoptosis and tumor regression in a human Calu 6

lung cancer xenograft model. Anticancer Drugs. 2011;22:454-62.

40. Yamanaka K, Nakahara T, Yamauchi T, Kita A, Takeuchi M, Kiyonaga F, et al. Antitumor activity of YM155, a selective small-molecule survivin suppressant, alone and in combination with docetaxel in human malignant melanoma models. Clin Cancer Res. 2011;17:5423-31.

41. Kaneko N, Kita A, Yamanaka K, Mori M. Combination of YM155, a survivin suppressant with a STAT3 inhibitor: a new strategy to treat diffuse large B-cell lymphoma. Leuk Res. 2013;37:1156-61.

42. Matasar MJ, Zelenetz AD. Overview of lymphoma diagnosis and management. Radiol Clin North Am. 2008;46:175-98, vii.

43. Rosenwald A, Wright G, Chan WC, Connors JM, Campo E, Fisher RI, et al. The use of molecular profiling to predict survival after chemotherapy for diffuse large-B-cell lymphoma. N Engl J Med. 2002;346:1937-47.

44. Lenz G, Wright G, Dave SS, Xiao W, Powell J, Zhao H, et al. Stromal gene signatures in large-B-cell lymphomas. N Engl J Med. 2008;359:2313-23.

45. Culpin RE, Proctor SJ, Angus B, Crosier S, Anderson JJ, Mainou-Fowler T. A 9 series microRNA signature differentiates between germinal centre and activated B-cell-like diffuse large B-cell lymphoma cell lines. Int J Oncol. 2010;37:367-76.

46. Aoyama Y, Nishimura T, Sawamoto T, Satoh T, Katashima M, Nakagawa K. Pharmacokinetics of sepantronium bromide (YM155), a small-molecule suppressor of survivin, in Japanese patients with advanced solid tumors: dose proportionality and influence of renal impairment. Cancer Chemother Pharmacol. 2012;70:373-80.

Fig. 1

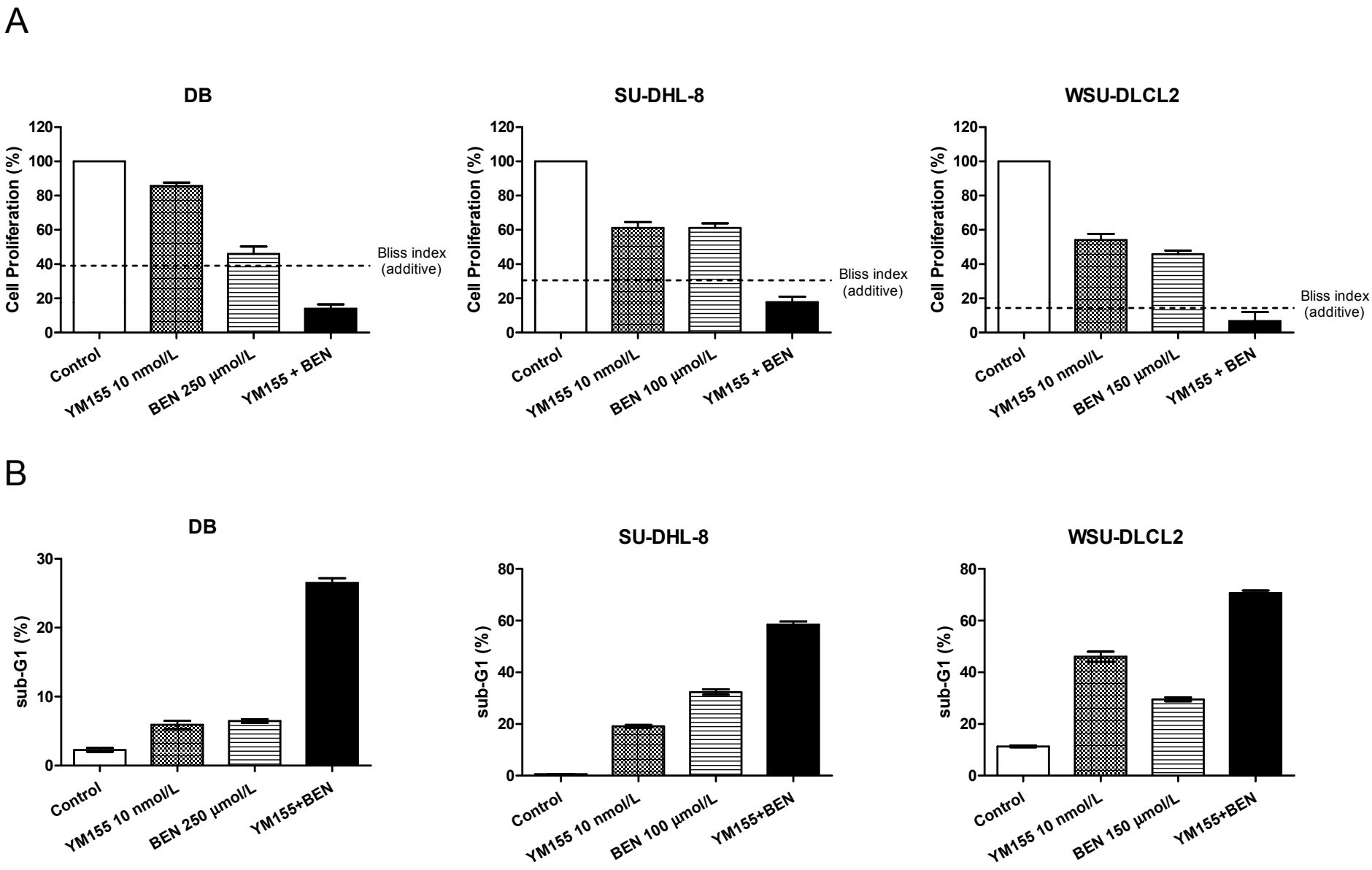

Fig. 2

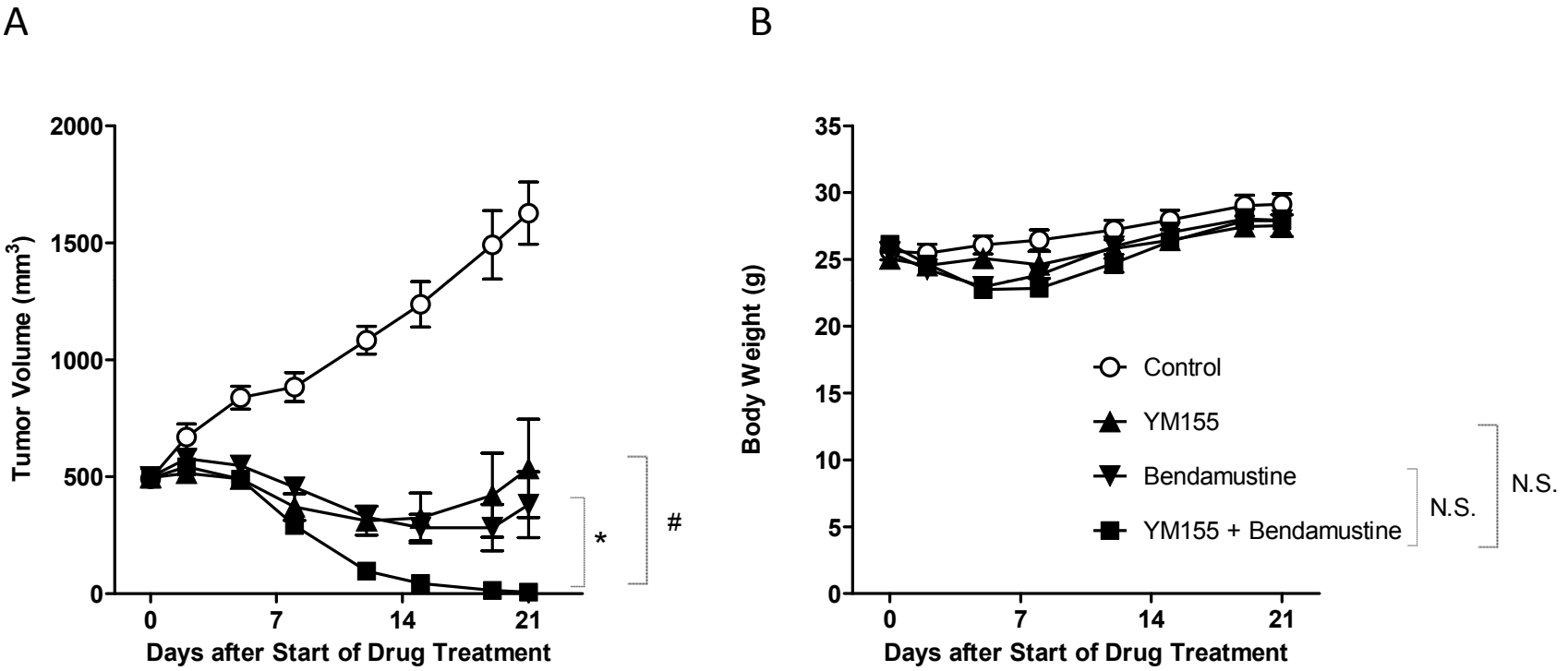

Fig. 3

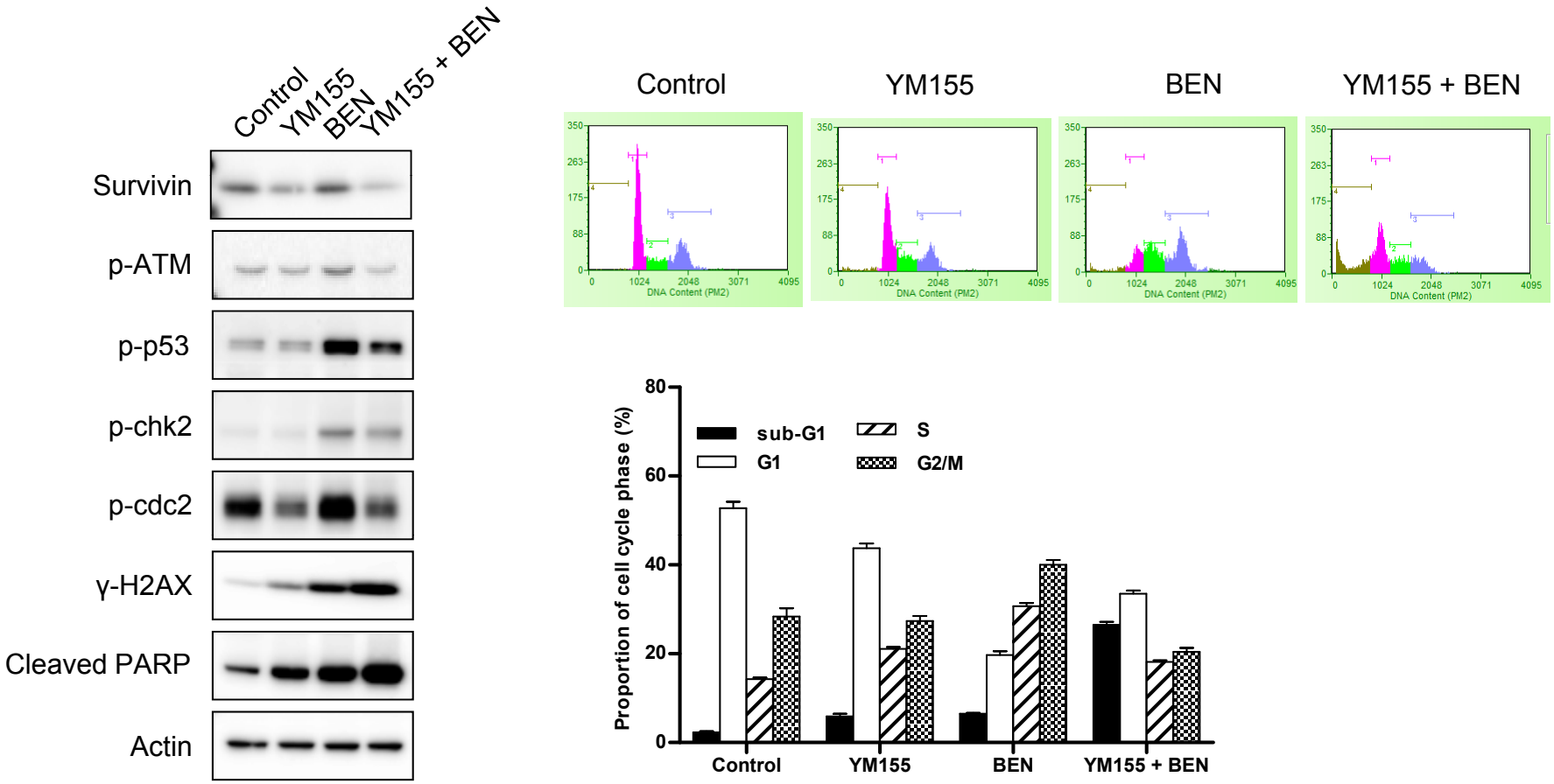

Fig. 4